

Three-dimensional reconstruction of magnetic resonance images of the anal sphincter and correlation between sphincter volume and pressure

Jeffrey L. Cornella, MD, Michael Hibner, MD, Dee E. Fenner, MD, J. Scott Kriegshauser, MD, Joseph Hentz, MS, and Javier F. Magrina, MD

Scottsdale, Ariz

OBJECTIVE: The purpose of this study was to assess the correlation between internal and external anal sphincter volumes and manometric anal pressures.

STUDY DESIGN: Ten healthy nulliparous women underwent anal sphincter magnetic resonance imaging and anal manometry measurement. A 3-dimensional reconstruction of magnetic resonance images was accomplished with the use of 3-dimensional slicer. Sphincter volumes were measured 3 times by the same observer for each of 10 patients. The intrarater reliability was measured with the use of the intraclass correlation coefficient ($ICC = \sigma^2_{\text{patients}} / (\sigma^2_{\text{patients}} + \sigma^2_{\text{error}})$) from a 2-way analysis of variance model with terms for patient and measurement trial. Measurements that were recorded on anal manometry included squeeze length, length of the high-pressure zone, and maximal resting and squeeze pressures.

RESULTS: The mean volumes (\pm SD) were 18.77 ± 4.64 cm³, 13.82 ± 3.8 cm³, and 32.36 ± 8.37 cm³ for internal, external, and combined sphincters, respectively. Intrarater reliability was 98% for external sphincter volume (95% CI, 94%-99%), 98% for internal sphincter volume (95% CI, 94%-99%), and 99% for total volume (95% CI, 97%-100%). On the 3-dimensional images, the internal sphincter was found to be cylindrical in shape, with an ellipse as a base. It is elongated in the anterior and posterior direction and flattened on the sides. The external sphincter was found to be funnel-shaped, being narrower caudad and widening in the cephalad direction. Similar to the internal sphincter, the external sphincter is elongated in the anteroposterior diameter. Volumes of the internal, external, and combined sphincters did not correlate with the maximum pressures at rest and squeeze. Correlations higher than $r = 0.5$ were observed for all 3 sphincter volume measurements versus high pressure zone at squeeze. The highest correlation, $r = 0.66$, was for internal sphincter volume versus high pressure zone at squeeze.

CONCLUSION: Three-dimensional reconstruction of the rectal sphincter musculature can be performed easily with 3-dimensional software. Measurements of the sphincter volumes have excellent intrarater reliability. Sphincter volumes do not correlate with pressures at rest or squeeze, but the internal sphincter volume correlates with the length of the high pressure zone at squeeze. Contrary to current generalized concepts, it is possible that the internal sphincter may play some role in generating the squeeze pressure. More research is necessary in applying 3-dimensional magnetic resonance image reconstruction in patients with different parity and continence status. Reconstruction of magnetic resonance images of the rectal sphincter musculature may prove to be beneficial in planning the treatment of patients with fecal incontinence. (*Am J Obstet Gynecol* 2003;189:130-5.)

Key words: Sphincter, manometry, magnetic resonance imaging

Pelvic floor muscles, fascia, and an intact nervous system play critical roles in fecal and urinary continence and pelvic organ support. Three-dimensional magnetic resonance imaging (MRI) is an excellent technique to visualize pelvic floor musculature in living humans. Since early

1990, multiple studies have been published that describe the use of MRI in pelvic floor assessment. In 1996, Strohehn et al¹ reported excellent correlation between cadaveric structures and MRI anatomy. Huddleston et al² reported alterations in vaginal shape that were associated with pelvic floor prolapse. Hoyte et al³ conducted studies about the correlation of 2- and 3-dimensional structure and volume and integrity of levator ani muscle in patients with urinary incontinence and pelvic organ prolapse. The authors showed the correlation of 2- and 3-dimensional measurements with continence status. Levator ani muscle volume was the highest in asymptomatic patients,

From Mayo Graduate School of Medicine.

Presented at the Twenty-Third Annual Meeting of the American Urogynecologic Society, San Francisco, California, October, 6-18, 2002.

Reprint requests: dodd.jeanne@mayo.edu

© 2003, Mosby, Inc. All rights reserved.

0002-9378/2003 \$30.00 + 0

doi:10.1067/mob.2003.545

Table I. Manometric parameters

| | <i>Maximum P_{rest} (mm Hg)</i> | <i>Max P_{squeeze} (mm Hg)</i> | <i>HPZ_{rest} (cm)</i> | <i>HPZ_{squeeze} (cm)</i> |
|------------|---|--|--------------------------------|-----------------------------------|
| Patient 1 | 161.0 | 199.1 | 3.3 | 3.4 |
| Patient 2 | 181.6 | 182.5 | 2.2 | 2.0 |
| Patient 3 | 136.0 | 150.4 | 3.9 | 3.3 |
| Patient 4 | 178.0 | 212.6 | 3.7 | 3.1 |
| Patient 5 | 126.2 | 195.5 | 2.4 | 3.3 |
| Patient 6 | 162.2 | 257.9 | 3.4 | 3.2 |
| Patient 7 | 81.1 | 215.9 | 2.5 | 2.6 |
| Patient 8 | 122.1 | 185.9 | 2.4 | 2.8 |
| Patient 9 | 184.6 | 209.4 | 2.8 | 2.2 |
| Patient 10 | 172.9 | 193.3 | 3.1 | 5.0 |

decreased in patients with genuine stress incontinence, and lowest in the group of patients with prolapse.

In 1998, we correlated MRI measurements of the anal sphincters with anal manometric-rectography pressure measurements in 10 normal women.⁴ Manometric pressures did not correlate with the muscle thickness along the sphincter. When the capability to perform 3-dimensional reconstruction of MRI images became available, it allowed us to use our original pressure data and MRI images to determine whether pressure correlated with sphincter volume.

Material and methods

This study was approved by Mayo Clinic Institutional Review Board, and all subjects gave written consent. Ten healthy, nulliparous female volunteers, between the ages of 21 and 40 years, participated in the study. All subjects were solicited through advertisement. Detailed medical, gynecologic, and colorectal histories were obtained before enrollment. The subjects were historically free of any previous anorectal trauma or surgery. Patients with history of gastrointestinal disease, fecal incontinence, obstipation, or medications that are known to affect gastrointestinal motility were excluded from the study. Patients who on physical examination had any evidence of trauma to the rectum or vagina or symptoms of neuropathy or in whom a pelvic mass was palpated were also excluded.

Thirty minutes before testing began, each patient received a Fleet's phosphate-soda enema (C.B. Fleet, Inc, Lynchburg, Va) and a tampon was placed in the vagina to improve MRI discrimination between vagina and rectum. Five patients had the manometry study done before MRI, and the remaining 5 patients had MRI done initially. The manometric studies were carried out in the gastrointestinal unit, and the MRI studies were carried out in the department of Radiology, Mayo Clinic Scottsdale. All MRI imaging was done by the same technician and read by the same investigator.

The manometric evaluation was accomplished by placing the patient in the left lateral decubitus position with knees and hips flexed. Anal pressure profiles were mea-

sured with a low compliant recording system SYNECTIC PC polygraph (version 5.0; Milford, Conn) and an 8-channel flexible catheter that was 4.8 mm optical density with a spiral and radial configuration of 8 ports. The catheter was perfused continuously with 25 μ L of distilled water per minute. Zero pressure calibration was done at the anal orifice level before insertion. The catheter was well lubricated, and no anesthesia was used throughout the procedure. After the insertion pressure was allowed to equalize for 10 seconds, 2 resting and 2 squeeze pressure profiles were obtained with the use of a continuous pull method with a rate of 1 mm per second (Table I).

The MRI was performed with a no. 10 pediatric catheter, the same diameter as the manometric probe, that was inserted into the anorectal canal at the exact location of the manometric catheter at its highest point during manometric evaluation. Each subject was supine in the MRI unit with a coupled dual 5-inch coil system positioned above and below the perineum. Scout images were obtained in the sagittal and coronal planes with the use of a spin echo (TE20/400TR) pulse sequence with 128 \times 256 matrix, a 24-cm field of view, and 1 number of excitations (NEX) or acquisition to ensure correct coil placement. These scout images were used to prescribe the sagittal sequence (TE6/35TR), 256 \times 256 matrix, 20-cm field of view, 2 NEX, 45-degree flip angle, and 3-mm thick contiguous slices. From the midsagittal image, oblique axial images that were perpendicular to the plane of the anal canal were obtained. Using a spin echo sequence (TE20/500TR) with 192 \times 256 matrix, a 20-cm field of view, 2 NEX, and 3-mm thick contiguous slices were obtained through the anorectal musculature. A third series of graphically prescribed images was made in a variable oblique fashion to image the plane of puborectalis. The same technical factors were used as axial obliques.

Three-dimensional reconstruction of the internal and external anal sphincter was done with a 3-dimensional Slicer (version 1.2.2; Massachusetts Institute of Technology/Harvard Medical School) installed on a personal computer. Slicer is open source software for visualization,

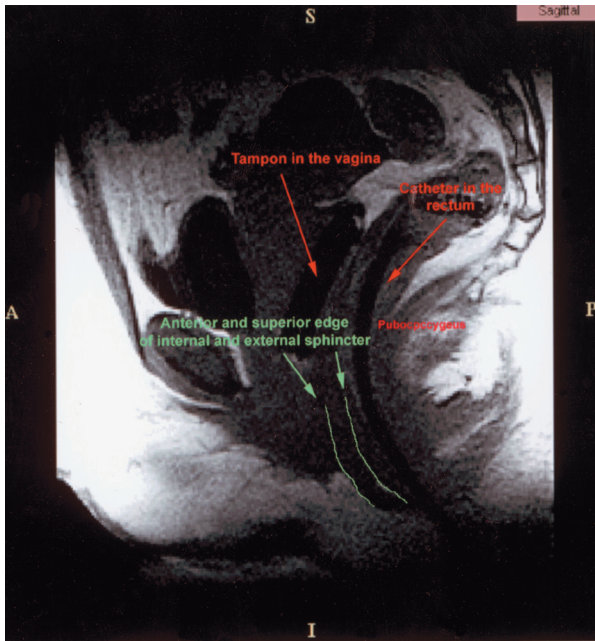


Fig 1. Sagittal view of the female pelvis and abdomen. The 2 green lines mark the anterior (A) and superior (S) border of the external and internal sphincter. P, posterior; I, inferior.

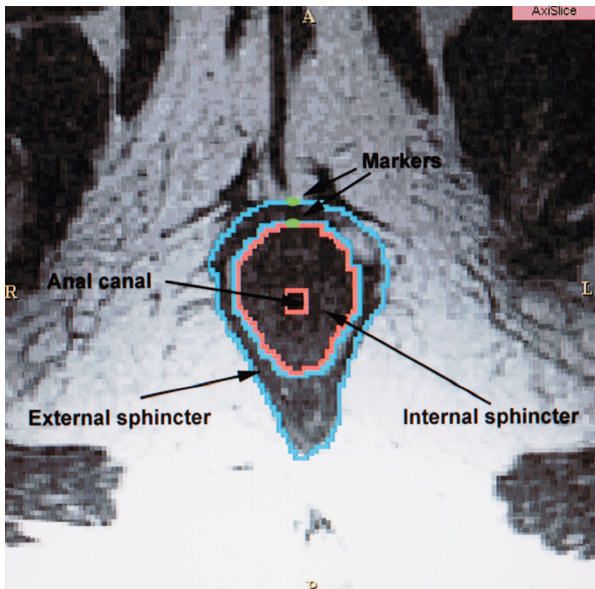


Fig 2. Axial view with outlined external (blue) and internal (red) sphincters. The anal canal is outlined (black) so that its volume can be subtracted from the volumes of internal and external sphincter.

registration, segmentation, and quantification of medical data, which was created in cooperation of Massachusetts Institute of Technology Artificial Intelligence Laboratory and Surgical Planning Laboratory at Brigham's Women's Hospital.

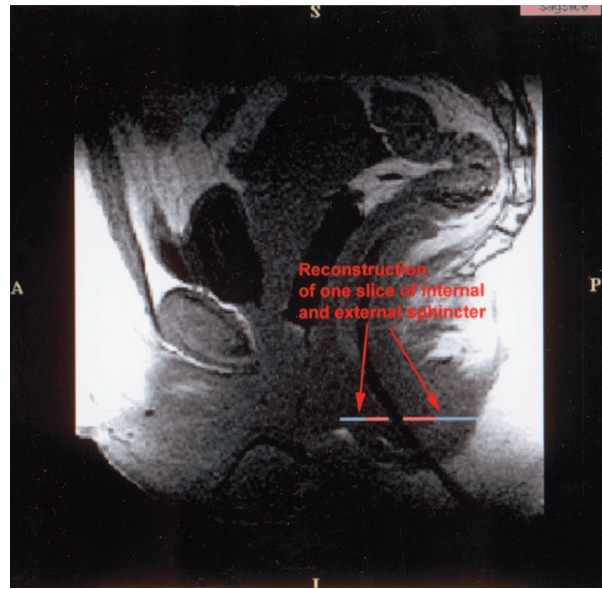


Fig 3. Sagittal view of slice depicted in Fig 2 (axial).

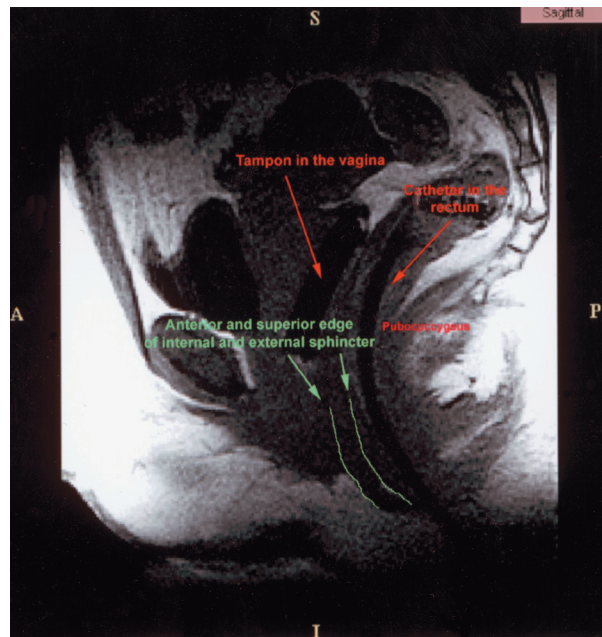


Fig 4. Reconstructed internal and external sphincter seen on the sagittal MRI image of the pelvis and abdomen.

Digital imaging and communications in medicine files that contain MRI images for each patient were obtained from the Department of Radiology and were transferred to a personal computer with Slicer installed. First, the midsagittal image for each patient was examined carefully. The anterior and superior border of the external anal sphincter and the border between external and internal sphincters were then marked (Fig 1). The view was switched to the oblique slices and, beginning from the

Table II. Measurements of internal and external sphincter

| | | Measurement (cm ³) | | | Average |
|------------|--------------------|--------------------------------|-------|-------|---------|
| | | 1 | 2 | 3 | |
| Patient 1 | External sphincter | 25.80 | 24.37 | 25.90 | 25.36 |
| | Internal sphincter | 17.07 | 17.86 | 17.78 | 17.57 |
| Patient 2 | External sphincter | 14.22 | 14.54 | 15.33 | 14.70 |
| | Internal sphincter | 10.68 | 10.23 | 10.70 | 10.53 |
| Patient 3 | External sphincter | 13.64 | 13.81 | 13.82 | 13.76 |
| | Internal sphincter | 11.07 | 11.16 | 10.17 | 10.80 |
| Patient 4 | External sphincter | 20.61 | 20.86 | 21.55 | 21.01 |
| | Internal sphincter | 16.73 | 17.27 | 18.30 | 17.43 |
| Patient 5 | External sphincter | 13.12 | 13.58 | 14.57 | 13.76 |
| | Internal sphincter | 9.97 | 10.21 | 10.95 | 10.38 |
| Patient 6 | External sphincter | 16.93 | 15.85 | 16.58 | 16.45 |
| | Internal sphincter | 13.70 | 13.32 | 12.91 | 13.31 |
| Patient 7 | External sphincter | 15.85 | 17.27 | 17.06 | 16.73 |
| | Internal sphincter | 11.10 | 11.57 | 11.22 | 11.30 |
| Patient 8 | External sphincter | 22.94 | 24.81 | 23.97 | 23.91 |
| | Internal sphincter | 17.15 | 17.74 | 17.43 | 17.44 |
| Patient 9 | External sphincter | 14.78 | 16.03 | 15.29 | 15.37 |
| | Internal sphincter | 9.80 | 9.59 | 9.25 | 9.55 |
| Patient 10 | External sphincter | 23.82 | 25.23 | 24.11 | 24.39 |
| | Internal sphincter | 18.82 | 20.51 | 20.26 | 19.86 |

Table III. Mean sphincter volumes

| | Mean volume (cm ³) | Intra-rater reliability (%) | 95% CI (%) |
|--------------------|--------------------------------|-----------------------------|------------|
| Internal sphincter | 13.82 ± 3.8 | 98 | 94-99 |
| External sphincter | 18.77 ± 4.6 | 98 | 94-99 |
| Total sphincter | 32.36 ± 8.3 | 99 | 97-100 |

most caudad slice on which muscle is seen, external anal sphincter (blue) and internal anal sphincter (red) were encircled (Figs 2 and 3). The anal canal with the pediatric catheter was also delimited so that the volume of the anal canal could be subtracted from the volume of the internal sphincter when the final calculation was done. This procedure was repeated until the most caudad edge of the sphincters was reached, which was manifested by a disappearance of the marker line from the axial slice. When all the slices were marked, the Slicer software performed a 3-dimensional reconstruction (Fig 4). The volumes of the internal and external sphincter were computed from reconstructed images. The total sphincter volume was calculated by the addition of the volumes of the internal and external sphincter.

Reconstruction of each of the patient images was performed 3 times, and the mean volumes of internal and external sphincters were calculated. The intrarater reliability was measured with the use of the intraclass correlation coefficient ($ICC = \sigma^2_{patients} / [\sigma^2_{patients} + \sigma^2_{error}]$) from a 2-way analysis of variance model with terms for patient and measurement trial.

Measurements that were recorded on anal manometry included squeeze length, length of the high-pressure zone,

Table IV. Correlation between sphincter volume and sphincter pressure (n = 10)

| Relationship | r | P value | 95% CI |
|-----------------------------------|------|---------|------------|
| External sphincter volume versus: | | | |
| Maximum pressure at rest | 0.13 | .73 | -0.55-0.70 |
| Maximum pressure at squeeze | 0.05 | .89 | -0.60-0.66 |
| HPZ at rest | 0.14 | .70 | -0.54-0.71 |
| HPZ at Squeeze | 0.50 | .14 | -0.18-0.86 |
| Internal sphincter volume versus | | | |
| Maximum pressure at rest | 0.19 | .60 | -0.50-0.73 |
| Maximum pressure at squeeze | 0.07 | .86 | -0.59-0.67 |
| HPZ at rest | 0.29 | .42 | -0.42-0.78 |
| HPZ at squeeze | 0.66 | .04 | 0.05-0.91 |
| Total sphincter volume vs | | | |
| Maximum pressure at rest | 0.16 | .65 | -0.52-0.72 |
| Maximum pressure at squeeze | 0.06 | .87 | -0.59-0.66 |
| HPZ at rest | 0.21 | .56 | -0.48-0.74 |
| HPZ at squeeze | 0.58 | .08 | -0.08-0.89 |

and maximal resting and squeeze pressures. *High pressure zone (HPZ) length* is defined as the length of the sphincter that generates pressure of $\geq 50\%$ of the mean pressure. The relationship between sphincter volumes and sphincter pressures was measured with the use of the Pearson correlation coefficient. Confidence intervals were calculated with the use of the Fisher Z-transformation.

Results

The mean volumes were 18.77 ± 4.64 cm³, 13.82 ± 3.8 cm³, and 32.36 ± 8.37 cm³ for the internal, external, and total sphincter respectively (Table II). The intrarater reliability was 98% for external sphincter volume (95% CI, 94%-99%), 98% for internal sphincter volume (95% CI,

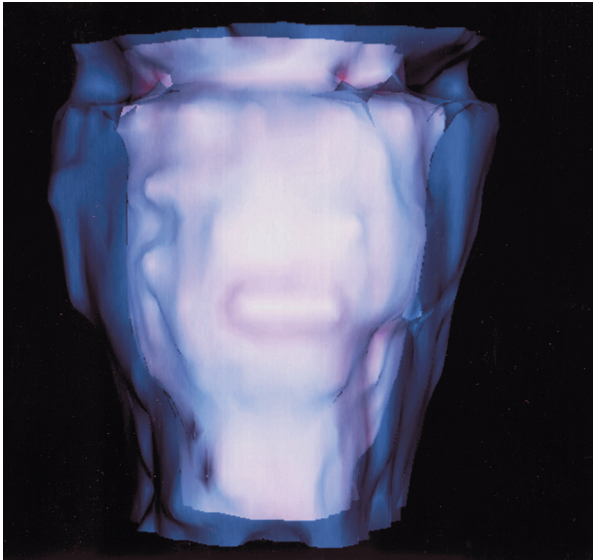


Fig 5. Anterior view of the reconstructed internal and external sphincters.

94%-99%), and 99% for total volume (95% CI, 97%-100%; Table III). On the 3-dimensional images the internal sphincter was found to be cylindrical in shape, with an ellipse as a base. It is elongated in the anterior and posterior direction and flattened on the sides.

The external sphincter was found to be funnel shaped (narrower caudad and widening in the cephalad direction). Similar to the internal sphincter, the external sphincter is elongated in the anteroposterior diameter (Figs 5 and 6).

The volumes of the internal, external, and total sphincter did not correlate with the maximum pressures at rest and squeeze (Table IV). Correlations higher than $r = .5$ were observed for all 3 sphincter volume measurements versus HPZ at squeeze (Table IV). The highest correlation, $r = .66$, was for the internal sphincter volume versus HPZ at squeeze (Fig 7). This finding is consistent with our previous report, which showed that the posterior sphincter length is correlated positively with the length of HPZ at squeeze.

Comment

Schafer et al⁵ correlated manometry with anal endosonography in 152 consecutive patients and found that maximum squeeze pressure was correlated significantly to muscle thickness of the external sphincter. There was no association found between the resting pressure and internal sphincter diameter. Sultan et al⁶ found no correlation between sphincter diameters and manometric pressures for either the internal or external sphincter.

Our original study showed no significant correlation between the manometric length and the anatomic length at rest. However, at squeeze, there was a positive correla-

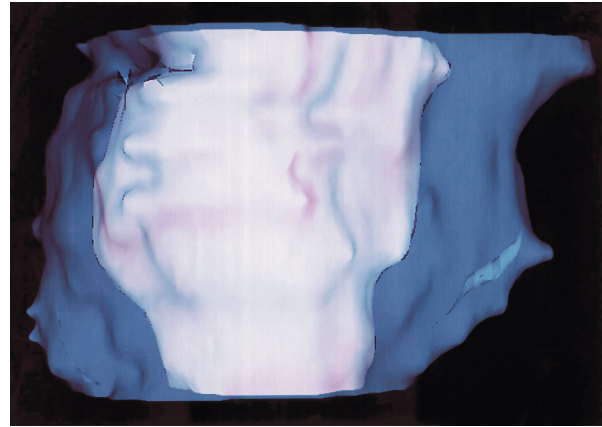


Fig 6. Left lateral view of the reconstructed internal and external sphincters.

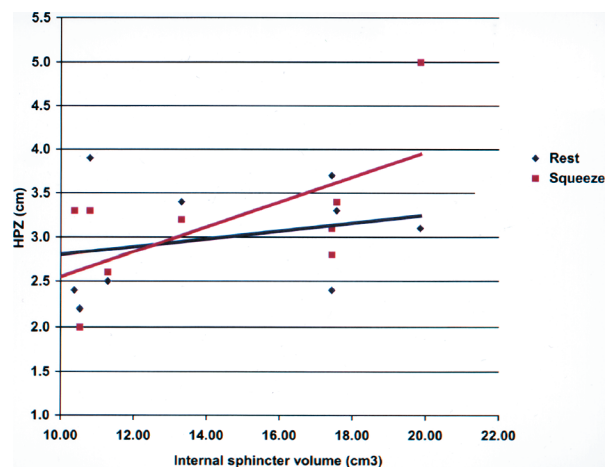


Fig 7. Relationship between internal sphincter volume and HPZ length at rest and at squeeze. The closed diamonds denote rest; the closed squares denote squeeze.

tion between the posterior length that was measured by MRI and the length of the HPZ with squeeze. This showed that the longer the posterior sphincter measured on MRI, the longer the HPZ measured on manometry. In the present study, a good correlation of the HPZ (manometric) length at squeeze with the internal sphincter (MRI) volume was found ($r^2 = 0.43$; $P = .037$). Pressure at squeeze has been attributed often to the external sphincter, with resting pressure that was attributed to the internal sphincter. The present study suggests that internal sphincter volume may also add to squeeze pressure.

The correlation between findings on imaging and clinical function is complex and may be impacted by ultrastructural factors that differ from patient to patient. Additional studies will be required to delineate which combination of anatomic and physiologic measurements result in an accurate predication of clinical function.

REFERENCES

1. Strohbehn K, Ellis J, Strohbehn JA, DeLancey JOL. Magnetic resonance imaging of the levator ani with anatomic correlations. *Obstet Gynecol* 1996;87:277-85.
2. Huddleston HT, Dunnihoo DT, Huddleston PM III, Meyers PC. Magnetic resonance imaging of defects in DeLancey's support levels I II and III. *Am J Obstet Gynecol* 1995;172:1778-84.
3. Hoyte L, Schierlitz L, Zou K, Flesh G, Fielding JR. Two- and three-dimensional MRI comparison of levator ani structure, volume and integrity in women with stress incontinence and prolapse. *Am J Obstet Gynecol* 2001;185:11-9.
4. Fenner DE, Kriegshauser SJ, Lee, HH, Beart RW, Weaver A, Cornella JL. Anatomic and physiologic measurements of the internal and external anal sphincters in normal females. *Obstet Gynecol* 1998;91:369-74.
5. Schafer R, Heyer T, Gantke B, Schafer A, Frieling T, Haussinger D, et al. Anal endosonography and manometry: comparison in patients with defecation problems. *Dis Colon Rect* 1997;40:293-7.
6. Sultan AH, Kamm MA, Hudson CN, Nicholls RJ, Bartram CI. Anal endosonography of the anal sphincters: normal anatomy and comparison with manometry. *Clin Radiol* 1994;49:368-74.